

# Multi-Agent Imitation Learning with Copulas

Hongwei Wang\* ✉, Lantao Yu\*, Zhangjie Cao, and Stefano Ermon

Computer Science Department, Stanford University, Stanford, CA 94305, USA  
{hongweiw, lantaoyu, caozj, ermon}@cs.stanford.edu

**Abstract.** Multi-agent imitation learning aims to train multiple agents to perform tasks from demonstrations by learning a mapping between observations and actions, which is essential for understanding physical, social, and team-play systems. However, most existing works on modeling multi-agent interactions typically assume that agents make independent decisions based on their observations, ignoring the complex dependence among agents. In this paper, we propose to use copula, a powerful statistical tool for capturing dependence among random variables, to explicitly model the correlation and coordination in multi-agent systems. Our proposed model is able to separately learn marginals that capture the local behavioral patterns of each individual agent, as well as a copula function that solely and fully captures the dependence structure among agents. Extensive experiments on synthetic and real-world datasets show that our model outperforms state-of-the-art baselines across various scenarios in the action prediction task, and is able to generate new trajectories close to expert demonstrations.

**Keywords:** multi-agent systems · imitation learning · copulas.

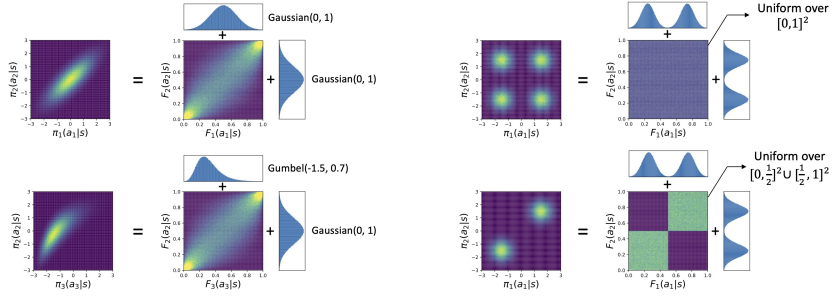
## 1 Introduction

Recent years have witnessed great success of reinforcement learning (RL) for single-agent sequential decision making tasks. As many real-world applications (e.g., multi-player games [27,6] and traffic light control [7]) involve the participation of multiple agents, multi-agent reinforcement learning (MARL) has gained more and more attention. However, a key limitation of RL and MARL is the difficulty of designing suitable reward functions for complex tasks with implicit goals (e.g., dialogue systems) [26,22,10,30]. Indeed, hand-tuning reward functions to induce desired behaviors becomes especially challenging in multi-agent systems, since different agents may have completely different goals and state-action representations [35].

Imitation learning [24,11] provides an alternative approach to directly programming agents by taking advantage of expert demonstrations on how a task should be solved. Although appealing, most prior works on multi-agent imitation learning typically assume agents make independent decisions after observing a state (i.e., mean-field factorization of the joint policy) [36,16,30,35], ignoring the

---

\* Equal contribution.



(a) Same copula but different marginals (b) Same marginals but different copulas

Fig. 1: In each subfigure, the left part visualizes the joint policy  $\pi(a_1, a_2|s)$  on the joint action space  $[-3, 3]^2$  and the right part shows the corresponding marginal policies (e.g.,  $\pi_1(a_1|s) = \int_{a_2} \pi(a_1, a_2|s) da_2$ ) as well as the copula  $c(F_1(a_1|s), F_2(a_2|s))$  on the unit cube. Here  $F_i$  is the cumulative distribution function of the marginal  $\pi_i(a_i|s)$  and  $u_i := F_i(a_i|s)$  is the uniformly distributed random variable obtained by probability integral transform with  $F_i$ . More details and definitions can be found in Section 3.1.

potentially complex dependencies that exist among agents. Recently, [33] and [19] proposed to implement correlated policies with opponent modeling, which incurs unnecessary modeling cost and redundancy, while still lacking coordination during execution.

Compared to the single-agent setting, one major and fundamental challenge in multi-agent learning is how to model the dependence among multiple agents in an effective and scalable way. Inspired by probability theory and statistical dependence modeling, in this work, we propose to use copulas [29,21,14] to model multi-agent behavioral patterns. Copulas are powerful statistical tools to describe the dependence among random variables, which have been widely used in quantitative finance for risk measurement and portfolio optimization [5]. Using a copulas-based multi-agent policy enables us to separately learn marginals that capture the local behavioral patterns of each individual agent and a copula function that only and fully captures the dependence structure among the agents. Such a factorization is capable of modeling arbitrarily complex joint policy and leads to *interpretable, efficient and scalable* multi-agent imitation learning. As a motivating example (see Fig. 1), suppose there are two agents, each with one-dimensional action space. In Fig. 1a, although two joint policies are quite different, they actually share the same copula (dependence structure) and one marginal. Our proposed copula-based policy is capable of capturing such information and more importantly, we may leverage such information to develop efficient algorithms for such transfer learning scenarios. For example, when we want to model team-play in a soccer game and one player is replaced by his/her substitute while the dependence among different roles are basically the same

regardless of players, we can immediately obtain a new joint policy by switching in the new player’s marginal while keeping the copula and other marginals unchanged. On the other hand, as shown in Fig. 1b, two different joint policies may share the same marginals while having different copulas, which implies that the mean-field policy in previous works (only modeling marginal policies and making independent decisions) cannot differentiate these two scenarios to achieve coordination correctly.

Towards this end, in this paper, we propose a copula-based multi-agent imitation learning algorithm, which is interpretable, efficient and scalable for modeling complex multi-agent interactions. Extensive experimental results on synthetic and real-world datasets show that our proposed method outperforms state-of-the-art multi-agent imitation learning methods in various scenarios and generates multi-agent trajectories close to expert demonstrations.

## 2 Preliminaries

We consider the problem of multi-agent imitation learning under the framework of Markov games [18], which generalize Markov Decision Processes to multi-agent settings, where  $N$  agents are interacting with each other. Specifically, in a Markov game,  $\mathcal{S}$  is the common state space,  $\mathcal{A}_i$  is the action space for agent  $i \in \{1, \dots, N\}$ ,  $\eta \in \mathcal{P}(\mathcal{S})$  is the initial state distribution and  $P : \mathcal{S} \times \mathcal{A}_1 \times \dots \times \mathcal{A}_N \rightarrow \mathcal{P}(\mathcal{S})$  is the state transition distribution of the environment that the agents are interacting with. Here  $\mathcal{P}(\mathcal{S})$  denotes the set of probability distributions over state space  $\mathcal{S}$ . Suppose at time  $t$ , agents observe  $s[t] \in \mathcal{S}$  and take actions  $\mathbf{a}[t] := (a_1[t], \dots, a_N[t]) \in \mathcal{A}_1 \times \dots \times \mathcal{A}_N$ , the agents will observe state  $s[t+1] \in \mathcal{S}$  at time  $t+1$  with probability  $P(s[t+1] \mid s[t], a_1[t], \dots, a_N[t])$ . In this process, the agents select the joint action  $\mathbf{a}[t]$  by sampling from a stochastic joint policy  $\boldsymbol{\pi} : \mathcal{S} \rightarrow \mathcal{P}(\mathcal{A}_1 \times \dots \times \mathcal{A}_N)$ . In the following, we will use subscript  $-i$  to denote all agents except for agent  $i$ . For example,  $(a_i, \mathbf{a}_{-i})$  represents the actions of all agents;  $\pi_i(a_i \mid s)$  and  $\pi_i(a_i \mid s, \mathbf{a}_{-i})$  represent the marginal and conditional policy of agent  $i$  induced by the joint policy  $\boldsymbol{\pi}(\mathbf{a} \mid s)$  (through marginalization and Bayes’ rule, respectively).

Suppose we have access to a set of demonstrations  $\mathcal{D} = \{\tau^j\}_{j=1}^M$  provided by some expert policy  $\boldsymbol{\pi}^E(\mathbf{a} \mid s)$ , where each expert trajectory  $\tau^j = \{(s^j[t], \mathbf{a}^j[t])\}_{t=1}^T$  is collected by the following sampling process:

$$s^1 \sim \eta(s), \mathbf{a}[t] \sim \boldsymbol{\pi}^E(\mathbf{a} \mid s[t]), s[t+1] \sim P(s[t+1] \mid s[t], \mathbf{a}[t]), \text{ for } t \geq 1.$$

The goal is to learn a parametric joint policy  $\boldsymbol{\pi}^\theta$  to approximate the expert policy  $\boldsymbol{\pi}^E$  such that we can do downstream inferences (e.g., action prediction and trajectory generation). The learning problem is off-line as we cannot ask for additional interactions with the expert policy or the environment during training, and the reward is also unknown.

### 3 Modeling Multi-Agent Interaction with Copulas

Many modeling methods for multi-agent learning tasks employ a simplifying mean-field assumption that the agents make independent action choices after observing a state [2,30,35], which means the joint policy can be factorized as follows:

$$\boldsymbol{\pi}(a_1, \dots, a_N | s) = \prod_{i=1}^N \pi_i(a_i | s). \quad (1)$$

Such a mean-field assumption essentially allows for independent construction of each agent’s policy. For example, multi-agent behavior cloning by maximum likelihood estimation is now equivalent to performing  $N$  single-agent behavior cloning tasks:

$$\max_{\boldsymbol{\pi}} \mathbb{E}_{(s, \mathbf{a}) \sim \rho_{\boldsymbol{\pi}_E}} [\log \boldsymbol{\pi}(\mathbf{a} | s)] = \sum_{i=1}^N \max_{\pi_i} \mathbb{E}_{(s, a_i) \sim \rho_{\boldsymbol{\pi}_E, i}} [\log \pi_i(a_i | s)], \quad (2)$$

where the occupancy measure  $\rho_{\boldsymbol{\pi}} : \mathcal{S} \times \mathcal{A}_1 \times \dots \times \mathcal{A}_N \rightarrow \mathbb{R}$  denotes the state action distribution encountered when navigating the environment using the joint policy  $\boldsymbol{\pi}$  [32,25] and  $\rho_{\boldsymbol{\pi}, i}$  is the corresponding marginal occupancy measure.

However, when the expert agents are making correlated action choices (e.g., due to joint plan and communication in a soccer game), such a simplifying modeling choice is not able to capture the rich dependency structure and coordination among agent actions. To address this issue, recent works [33,19] propose to use a different factorization of the joint policy such that the dependency among  $N$  agents can be preserved:

$$\boldsymbol{\pi}(a_i, \mathbf{a}_{-i} | s) = \pi_i(a_i | s, \mathbf{a}_{-i}) \boldsymbol{\pi}_{-i}(\mathbf{a}_{-i} | s), \text{ for } i \geq 1. \quad (3)$$

Although such a factorization is general and captures the dependency among multi-agent interactions, several issues still remain. First, the modeling cost is increased significantly, because now we need to learn  $N$  different and complicated opponent policies  $\boldsymbol{\pi}_{-i}(\mathbf{a}_{-i} | s)$  as well as  $N$  different marginal conditional policies  $\pi_i(a_i | s, \mathbf{a}_{-i})$ , each with a deep neural network. It should be noted that there are many redundancies in such a modeling choice. Specifically, suppose there are  $N$  agents and  $N > 3$ , for agent 1 and  $N$ , we need to learn opponent policies  $\boldsymbol{\pi}_{-1}(a_2, \dots, a_N | s)$  and  $\boldsymbol{\pi}_{-N}(a_1, \dots, a_{N-1} | s)$  respectively. These are potentially high dimensional and might require flexible function approximations. However, the dependency structure among agent 2 to agent  $N - 1$  are modeled in both  $\boldsymbol{\pi}_{-1}$  and  $\boldsymbol{\pi}_{-N}$ , which incurs unnecessary modeling cost. Second, when executing the policy, each agent  $i$  makes decisions through its marginal policy  $\pi_i(a_i | s) = \mathbb{E}_{\boldsymbol{\pi}_{-i}(\mathbf{a}_{-i} | s)}(\pi_i(a_i | s, \mathbf{a}_{-i}))$  by first sampling  $\mathbf{a}_{-i}$  from its opponent policy  $\boldsymbol{\pi}_{-i}$  then sampling its action  $a_i$  from  $\pi_i(\cdot | s, \mathbf{a}_{-i})$ . Since each agent is performing such decision process independently, coordination among agents are still impossible due to sampling randomness. Moreover, a set of independently learned conditional distributions are not necessarily consistent with each other (i.e., induced by the same joint policy) [35].

In this work, to address above challenges, we draw inspiration from probability theory and propose to use copulas, a statistical tool for describing the dependency structure between random variables, to model the complicated multi-agent interactions in a scalable and efficient way.

### 3.1 Copulas

When the components of a multivariate random variable  $\mathbf{x} = (x_1, \dots, x_N)$  are jointly independent, the density of  $\mathbf{x}$  can be written as:

$$p(\mathbf{x}) = \prod_{i=1}^N p(x_i). \quad (4)$$

When the components are not independent, this equality does not hold any more as the dependencies among  $x_1, \dots, x_N$  can not be captured by the marginals  $p(x_i)$ . However, the differences can be corrected by multiplying the right hand side of Equation (4) with a function that *only and fully* describes the dependency. Such a function is called a copula [21], a multivariate distribution function on the unit hyper-cube with uniform marginals.

Intuitively, consider a random variable  $x_i$  with continuous cumulative distribution function  $F_i$ . Applying *probability integral transform* gives us a random variable  $u_i = F_i(x_i)$ , which has standard uniform distribution. Thus one can use this property to separate the information in marginals from the dependency structures among  $x_1, \dots, x_N$  by first projecting each marginal onto one axis of the hyper-cube and then capture the pure dependency with a distribution on the unit hyper-cube.

Formally, a copula is the joint distribution of random variables  $u_1, \dots, u_N$ , each of which is marginally uniformly distributed on the interval  $[0, 1]$ . Furthermore, we introduce the following theorem that provides the theoretical foundations of copulas:

**Theorem 1 (Sklar’s Theorem [28]).** *Suppose the multivariate random variable  $(x_1, \dots, x_N)$  has marginal cumulative distribution functions  $F_1, \dots, F_N$  and joint cumulative distribution function  $F$ , then there exists a unique copula  $C : [0, 1]^N \rightarrow [0, 1]$  such that:*

$$F(x_1, \dots, x_N) = C(F_1(x_1), \dots, F_N(x_N)). \quad (5)$$

*When the multivariate distribution has a joint density  $f$  and marginal densities  $f_1, \dots, f_N$ , we have:*

$$f(x_1, \dots, x_N) = \prod_{i=1}^N f_i(x_i) \cdot c(F_1(x_1), \dots, F_N(x_N)), \quad (6)$$

*where  $c$  is the probability density function of the copula. The converse is also true. Given a copula  $C$  and marginals  $F_i(x_i)$ , then  $C(F_1(x_1), \dots, F_N(x_N)) = F(x_1, \dots, x_N)$  is a  $N$ -dimensional cumulative distribution function with marginal distributions  $F_i(x_i)$ .*

Theorem 1 states that every multivariate cumulative distribution function  $F(x_1, \dots, x_N)$  can be expressed in terms of its marginals  $F_i(x_i)$  and a copula  $C(F_1(x_1), \dots, F_N(x_N))$ . Comparing Eq. (4) with Eq. (6), we can see that a copula function encoding correlations between random variables can be used to correct the mean-field approximation for arbitrarily complex distribution.

### 3.2 Multi-Agent Imitation Learning with Copulas

A central question in multi-agent imitation learning is how to model the dependency structure among agent decisions properly. As discussed above, the framework of copulas provides a mechanism to decouple the marginal policies (individual behavioral patterns) from the dependency left in the joint policy after removing the information in marginals. In this work, we advocate copula-based policy for multi-agent learning because copulas offer unique and desirable properties in multi-agent scenarios. For example, suppose we want to model the interactions among players in a soccer game. By using copulas, we will obtain marginal policies for each individual player as well as dependencies among different roles (e.g., forwards and midfielders). Such a multi-agent learning framework has the following advantages:

- **Interpretable.** The learned copula density can be easily visualized to intuitively analyze the correlation among agent actions.
- **Scalable.** When the marginal policy of agents changes but the dependency among different agents remain the same (e.g., in a soccer game, one player is replaced by his/her substitute, but the dependence among different roles are basically the same regardless of players), we can obtain a new joint policy efficiently by switching in the new agent’s marginal while keeping the copula and other marginals unchanged.
- **Succinct.** The copula-based factorization of the joint policy avoids the redundancy in previous opponent modeling approaches [33,19] by separately learning marginals and a copula.

**Learning.** We first discuss how to learn a copula-based policy from a set of expert demonstrations. Under the framework of Markov games and copulas, we factorize the parametric joint policy as:

$$\boldsymbol{\pi}(a_1, \dots, a_N | s; \boldsymbol{\theta}) = \prod_{i=1}^N \pi_i(a_i | s; \theta_i) \cdot c(F_1(a_1 | s; \theta_1), \dots, F_N(a_N | s; \theta_N) | s; \theta_c), \quad (7)$$

where  $\pi_i(a_i | s; \theta_i)$  is the marginal policy of agent  $i$  with parameters  $\theta_i$  and  $F_i$  is the corresponding cumulative distribution function; the function  $c$  (parameterized by  $\theta_c$ ) is the density of the copula on the transformed actions  $u_i = F_i(a_i | s; \theta_i)$  obtained by processing original actions with probability integral transform.

The training algorithm of our proposed method is presented as Algorithm 1. Given a set of expert demonstrations  $\mathcal{D}$ , our goal is to learn marginal actions of

**Algorithm 1:** Training procedure

---

**Input:** The number of trajectories  $M$ , the length of trajectory  $T$ , the number of agents  $N$ , demonstrations  $\mathcal{D} = \{\tau^i\}_{i=1}^M$ , where each trajectory  $\tau^i = \{(s^i[t], \mathbf{a}^i[t])\}_{t=1}^T$

**Output:** Marginal action distribution MLP  $MLP_{marginal}$ , state-dependent copula MLP  $MLP_{copula}$  or state-independent copula density  $c(\cdot)$

```

// Learning marginals
1 while  $MLP_{marginal}$  not converge do
2   for each state-action pair  $(s, (a_1, \dots, a_N))$  do
3     Calculate the conditional marginal action distributions for all agents:
4      $\{f_j(\cdot|s)\}_{j=1}^N \leftarrow MLP_{marginal}(s)$ ;
5     for agent  $j = 1, \dots, N$  do
6       Calculate the likelihood of the observed action  $a_j$ :  $f_j(a_j|s)$ ;
7       Maximize  $f_j(a_j|s)$  by optimizing  $MLP_{marginal}$  using SGD;

// Learning copula
8 while  $MLP_{copula}$  or  $c(\cdot)$  not converge do
9   for each state-action pair  $(s, (a_1, \dots, a_N))$  do
10     $\{f_j(\cdot|s)\}_{j=1}^N \leftarrow MLP_{marginal}(s)$ ;
11    for agent  $j = 1, \dots, N$  do
12       $F_j(\cdot|s) \leftarrow$  the CDF of  $f_j(\cdot|s)$ ;
13      Transform  $a_j$  to uniformly distributed value:  $u_j \leftarrow F_j(a_j|s)$ ;
14      Obtain  $u = (u_1, \dots, u_N) \in [0, 1]^N$ ;
15      if copula is set as state-dependent then
16        Calculate the copula density  $c(\cdot|s) \leftarrow MLP_{copula}(s)$ ;
17        Calculate the likelihood of  $u$ :  $c(u|s)$ ;
18        Optimize  $MLP_{copula}$  by maximizing  $\log c(u|s)$  using SGD;
19      else
20        Calculate the likelihood of  $u$ :  $c(u)$ ;
21        Optimize parameters of  $c(\cdot)$  using maximum likelihood or
        non-parametric methods;

22 return  $MLP_{marginal}$ ,  $MLP_{copula}$  or  $c(\cdot)$ 

```

---

agents and their copula function. Our approach consists of two steps.<sup>1</sup> We first learn marginal action distributions of each agent given their current state (lines 1-6). This is achieved by training  $MLP_{marginal}$  that takes as input a state  $s$  and output the parameters of marginal action distributions of  $N$  agents given the input state (line 3).<sup>2</sup> In our implementation, we use mixture of Gaussians to realize

<sup>1</sup> An alternate approach is to combine the two steps together and use end-to-end training, but this does not perform well in practice because the copula term is unlikely to converge before marginals are well-trained.

<sup>2</sup> Here we assume that each agent is aware of the whole system state. But our model can be easily generalized to the case where agents are only aware of partial system state by feeding the corresponding state to their MLPs.

each marginal policy  $\pi_i(a_i|s; \theta_i)$  such that we can model complex multi-modal marginals while having a tractable form of the marginal cumulative distribution functions. Therefore, the output of  $MLP_{marginal}$  consists of the means, covariance, and weights of components for the  $N$  agents’ Gaussian mixtures. We then calculate the likelihood of each observed action  $a_j$  based on agent  $j$ ’s marginal action distribution (line 5), and maximize the likelihood by optimizing the parameters of  $MLP_{marginal}$  (line 6).

After learning marginals, we fix the parameters of marginal MLPs and start learning the copula (lines 7-20). We first process the original demonstrations using probability integral transform and obtain a set of new demonstrations with uniform marginals (lines 8-13). Then we learn the density of copula (lines 14-20). Notice that the copula can be implemented as either *state-dependent* (lines 14-17) or *state-independent* (lines 18-20): For state-dependent copula, we use  $MLP_{copula}$  to take as input the current state  $s$  and outputs the parameters of copula density  $c(\cdot|s)$  (line 15). Then we calculate the likelihood of copula value  $u$  (line 16) and maximize the likelihood by updating  $MLP_{copula}$  (line 17). For state-independent copula, we directly calculate the likelihood of copula value  $u$  under  $c(\cdot)$  (line 19) and learn parameters of  $c(\cdot)$  by maximizing the likelihood of copula value (line 20).

The copula density ( $c(\cdot)$  or  $c(\cdot|s)$ ) can be implemented using parametric methods such as Gaussian or mixture of Gaussians. It is worth noticing that if copula is state-independent, it can also be implemented using non-parametric methods such as kernel density estimation [23,8]. In this way, we no longer learn parameters of copula by maximizing likelihood as in lines 19-20, but simply store all copula values  $u$  for density estimation and sampling in inference stage. We will visualize the learned copula in experiments.

**Inference.** In inference stage, the goal is to predict the joint actions of all agents given their current state  $s$ . The inference algorithm is presented as Algorithm 2, where we first sample a copula value  $u = (u_1, \dots, u_N)$  from the learned copula, either state-dependent or state-independent (lines 1-5), then apply inverse probability transform to transform them to the original action space:  $\hat{a}_j = F_j^{-1}(u_j|s)$  (lines 7-10). Note that an analytical form of the inverse cumulative distribution function may not always be available. In our implementation, we use binary search to approximately solve this problem since  $F_j$  is a strictly increasing function, which is shown to be highly efficient in practice. In addition, we can also sample multiple i.i.d. copula values from  $c(\cdot|s)$  or  $c(\cdot)$  (line 3 or 5), transform them into the original action space, and take their average as the predicted action. This strategy is shown to be able to improve the accuracy of action prediction (in terms of MSE loss), but requires more running time as a trade-off.

**Generation.** The generation algorithm is presented as Algorithm 3. To generate new trajectories, we repeatedly predict agent actions given the current state (line 2), then execute the generated action and obtain an updated state from the environment (line 3).

**Complexity Analysis.** The computational complexity of the training and the inference algorithms is analyzed as follows. The complexity of each round in



---

**Algorithm 2:** Inference procedure

---

**Input:** Marginal action distribution MLP  $MLP_{marginal}$ , state-dependent copula MLP  $MLP_{copula}$  or state-independent copula density  $c(\cdot)$ , current state  $s$

**Output:** Predicted action  $\hat{a}$

// Sample from copula

- 1 **if** *copula is set as state-dependent* **then**
- 2   | Calculate (parameters of) state-dependent copula density  
     $c(\cdot|s) \leftarrow MLP_{copula}(s)$ ;
- 3   | Sample a copula value  $u = (u_1, \dots, u_N)$  from  $c(\cdot|s)$ ;
- 4 **else**
- 5   | Sample a copula value  $u = (u_1, \dots, u_N)$  from  $c(\cdot)$ ;
- // Transform copula value to action space
- 6 Calculate (parameters of) the conditional marginal action distributions for all agents:  $\{f_j(\cdot|s)\}_{j=1}^N \leftarrow MLP_{marginal}(s)$ ;
- 7 **for** agent  $j = 1, \dots, N$  **do**
- 8   |  $F_j(\cdot|s) \leftarrow$  CDF of  $f_j(\cdot|s)$ ;
- 9   |  $\hat{a}_j \leftarrow F_j^{-1}(u_j|s)$ ;
- 10  $\hat{a} \leftarrow (\hat{a}_1, \dots, \hat{a}_j)$ ;
- 11 **return**  $\hat{a}$

---



---

**Algorithm 3:** Generation procedure

---

**Input:** Inference module (Algorithm 2), initial state  $s[0]$ , required length  $L$ , environment  $\mathcal{E}$

**Output:** Generated trajectory  $\hat{\tau}$

- 1 **for**  $l = 0, \dots, L$  **do**
- 2   | Feed state  $s[l]$  to the inference module and get the predicted action  $\hat{a}[l]$ ;
- 3   | Execute  $\hat{a}[l]$  in environment  $\mathcal{E}$  and get a new state  $s[l + 1]$ ;
- 4  $\hat{\tau} = \{(s[l], \hat{a}[l])\}_{l=0}^L$ ;
- 5 **return**  $\hat{\tau}$ ;

---

Algorithm 1 is  $O(MTN)$ , where  $M$  is the number of trajectories in the training set,  $T$  is the length of each trajectory, and  $N$  is the number of agents. The complexity of Algorithm 2 is  $O(N)$ . The training and the inference algorithms scales linearly with the size of input dataset.

## 4 Related Work

The key problem in multi-agent imitation learning is how to model the dependence structure among multiple agents. [16] learn a latent coordination model for players in a cooperative game, where different players occupy different roles. However, there are many other multi-agent scenarios where agents do not cooperate for a same goal or they do not have specific roles (e.g., self-driving). [4] adopt parameter



Fig. 2: Experimental environments: PhySim, Driving, and RoboCup.

sharing trick to extend generative adversarial imitation learning to handle multi-agent problems, but it does not model the interaction of agents. Interaction Network [3] learns a physical simulation of objects with binary relations, and CommNet [31] learns dynamic communication among agents. But they fail to characterize the dependence among agent actions explicitly.

Researchers also propose to infer multi-agent relationship using graph techniques or attention mechanism. For example, [15] propose to use graph neural networks (GNN) to infer the type of relationship among agents. [12] introduces attention mechanism into multi-agent predictive modeling. [17] combine generative models and attention mechanism to capture behavior generating process of multi-agent systems. These works address the problem of reasoning relationship among agents rather than capturing their dependence when agents are making decisions.

Another line of related work is deep generative models in multi-agent systems. For example, [36] propose a hierarchical framework with programmatically produced weak labels to generate realistic multi-agent trajectories of basketball game. [34] use GNN and variational recurrent neural networks (VRNN) to design a permutation equivariant multi-agent trajectory generation model for sports games. [13] combine conditional variational autoencoder (CVAE) and long-short term memory networks (LSTM) to generate behavior of basketball players. Most of the existing works focus on agent behavior forecasting but provide limited information regarding the dependence among agent behaviors.

## 5 Experiments

### 5.1 Experimental Setup

**Datasets.** We evaluate our method in three settings. **PhySim** is a synthetic physical environment where 5 particles are connected by springs. **Driving** is a synthetic driving environment where one vehicle follows another along a single lane. **RoboCup** is collected from an international scientific robot competition where two robot teams (including 22 robots) compete against each other. Experimental environments are shown in Fig. 2. The detailed dataset description is provided in Appendix A.

**Baselines.** We compare our method with the following baselines: **LR** is a logistic regression model that predicts actions of agents using all of their states. **SocialLSTM** [1] predicts agent trajectory using RNNs with a social pooling

Table 1: Root mean squared error (RMSE) between predicted actions and ground-truth actions for all methods.

Methods	PhySim	Driving	RoboCup
<b>LR</b>	$0.064 \pm 0.002$	$0.335 \pm 0.007$	$0.478 \pm 0.009$
<b>SocialLSTM</b>	$0.186 \pm 0.032$	$0.283 \pm 0.024$	$0.335 \pm 0.051$
<b>IN</b>	$0.087 \pm 0.013$	$0.247 \pm 0.033$	$0.320 \pm 0.024$
<b>CommNet</b>	$0.089 \pm 0.007$	$0.258 \pm 0.028$	$0.311 \pm 0.042$
<b>VAIN</b>	$0.082 \pm 0.010$	$0.242 \pm 0.031$	$0.315 \pm 0.028$
<b>NRI</b>	$0.055 \pm 0.011$	$0.296 \pm 0.018$	$0.401 \pm 0.042$
<b>Copula</b>	<b><math>0.037 \pm 0.005</math></b>	<b><math>0.158 \pm 0.019</math></b>	<b><math>0.221 \pm 0.024</math></b>

layer in the hidden state of nearby agents. **IN** [3] predicts agent states and their interactions using deep neural networks. **CommNet** [31] simulates the inter-agent communication by broadcasting the hidden states of all agents and then predicts their actions. **VAIN** [12] uses neural networks with attention mechanism for multi-agents modeling. **NRI** [15] designs a graph neural network based model to learn the interaction type among multiple agents. Since most of the baselines are used for predicting future states given historical state, we change the implementation of their objective functions and use them to predict the current action of agents given historical states. Each experiment is repeated 3 times, and we report the mean and standard deviation. Hyper-parameter settings of baselines as well as our method are presented in Appendix B.

## 5.2 Results

We compare our method with baselines in the task of action prediction. The results of root mean squared error (RMSE) between predicted actions and ground-truth actions are presented in Table 1. The number of Gaussian mixture components in our method is set to 2 for all datasets. The results demonstrate that all methods performs the best on PhySim dataset, since agents in PhySim follow simple physical rules and the relationships among them are linear thus easy to infer. However, the interactions of agents in Driving and RoboCup datasets are more complicated, which causes LR and NRI to underperform other baselines. The performance of IN, CommNet, and VAIN are similar, which is in accordance with the result reported in [12]. Our method is shown to outperform all baselines significantly on all three datasets, which demonstrates that explicitly characterizing dependence of agent actions could greatly improve the performance of multi-agent behavior modeling.

To investigate the efficacy of copula, we implement three types of copula function: Uniform copula means we do not model dependence among agent actions. KDE copula uses kernel density estimation to model the copula function, which is state-independent. Gaussian mixtures copula uses Gaussian mixture model to characterize the copula function, of which the parameters are output by an MLP taking as input the current state. We train the three models on training

Table 2: Negative log-likelihood (NLL) of test trajectories evaluated by different types of copula. Uniform copula assumes no dependence among agent actions. KDE copula uses kernel density estimation to model the copula, which is state-independent. Gaussian mixtures copula uses Gaussian mixture model to characterize the copula, which is state-dependent.

Copula type	PhySim	Driving	RoboCup
<b>Uniform</b>	$8.994 \pm 0.001$	$-0.571 \pm 0.024$	$3.243 \pm 0.049$
<b>KDE</b>	<b><math>1.256 \pm 0.006</math></b>	<b><math>-0.916 \pm 0.017</math></b>	<b><math>0.068 \pm 0.052</math></b>
<b>Gaussian mixture</b>	$2.893 \pm 0.012$	$-0.621 \pm 0.028$	$3.124 \pm 0.061$

Combinations	PhySim	Driving	RoboCup
<b>Old marginals + old copula</b>	$10.231 \pm 0.562$	$15.184 \pm 1.527$	$4.278 \pm 0.452$
<b>Old marginals + new copula</b>	$8.775 \pm 0.497$	$13.662 \pm 0.945$	$4.121 \pm 0.658$
<b>New marginals + old copula</b>	$1.301 \pm 0.016$	$0.447 \pm 0.085$	$0.114 \pm 0.020$
<b>New marginals + new copula</b>	$1.259 \pm 0.065$	$-0.953 \pm 0.024$	$0.077 \pm 0.044$

Table 3: Negative log-likelihood (NLL) of new test trajectories in which the action distribution of one agent is changed. We evaluate the new test trajectories based on whether to use the old marginal action distributions or copula, which results in four combinations.

trajectories, then calculate negative log-likelihood (NLL) of test trajectories using the three trained models. A lower NLL score means that the model assigns high likelihood to given trajectories, showing that it is better at characterizing the dataset. The NLL scores of the three models on the three datasets are reported in Table 2. The performance of KDE copula and Gaussian copula both surpasses uniform copula, which demonstrates that modeling dependence among agent actions is essential for improving model expressiveness. However, Gaussian copula performs worse than KDE copula, because Gaussian copula is state-dependent thus increases the risk of overfitting. Notice that the performance gap between KDE and Gaussian copula is less on PhySim, since PhySim dataset is much larger so the Gaussian copula can be trained more effectively.

### 5.3 Generalization of Copula

One benefit of copulas is that copula captures the pure dependence among agents, regardless of their own marginal action distributions. To demonstrate the generalization capabilities of copulas, we design the following experiment. We first train our model on the original dataset, and learn marginal action distributions and copula function (which is called *old marginals* and *old copula*). Then we substitute one of the agents with a new agent and use the simulator to generate a new set of trajectories. Specifically, this is achieved by doubling the action value of one agent (for example, this can be seen as substituting an existing particle with a lighter one in PhySim). We retrain our model on new trajectories and learn *new marginals* and *new copula*. We evaluate the likelihood of new trajectories based on

whether to use the old marginals or old copula, which, accordingly, results in four combinations. The NLL scores of four combinations are presented in Table 3. It is clear, by comparing the first and the last row, that “new marginals + new copula” significantly outperform “old marginals + old copula”, since new marginals and new copula are trained on new trajectories and therefore characterize the new joint distribution exactly. To see the influence of marginals and copula more clearly, we further compare the results in row 2 and 3, where we use new copula or new marginals separately. It is clear that the model performance does not drop significantly if we use the old copula and new marginals (by comparing row 3 and 4), which demonstrates that the copula function basically stays the same even if marginals are changed. The result supports our claim that the learned copula is generalizable in the case where marginal action distributions of agents change but the internal inter-agent relationship stays the same.

#### 5.4 Copula Visualization

Another benefit of copulas is that it is able to intuitively demonstrate the correlation among agent actions. We choose the RoboCup dataset to visualize the learned copula. As shown in Fig. 3a, we first randomly select a game (the 6th game) between cyrus2017 and helios2017 and draw trajectories of 10 players in the left team (L2  $\sim$  L11, except the goalkeeper). It is clear that the 10 players fulfill specific roles: L2  $\sim$  L4 are defenders, L5  $\sim$  L8 are midfielders, and L9  $\sim$  L11 are forwards. Then we plot the copula density between the x-axis (the horizontal direction)

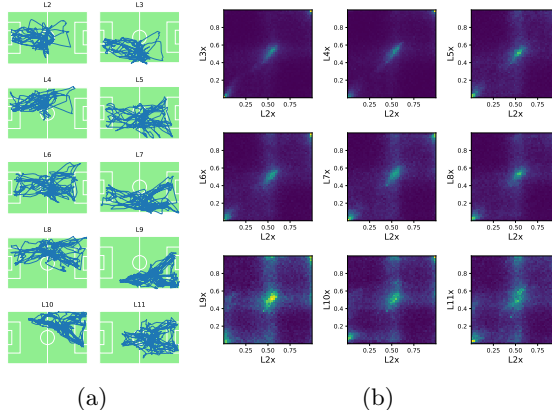


Fig. 3: (a) Trajectories of 10 players (except the goalkeeper) of the left team in one RoboCup game; (b) Copula density between x-axis of L2 and x-axis of another player (L3  $\sim$  L11).

of L2 and the x-axis of L3  $\sim$  L11, respectively, as shown in Fig. 3b. These figures illustrate linear correlation between their moving direction along x-axis, that is, when L2 moves forward other players are also likely to move forward. However, the correlation strength differs with respect to different players: L2 exhibits high correlation with L3 and L4, but low correlation with L9  $\sim$  L11. This is because L2  $\sim$  L4 are all defenders so they collaborate more closely with each other, but L9  $\sim$  L11 are forwards thus far from L2 in the field.

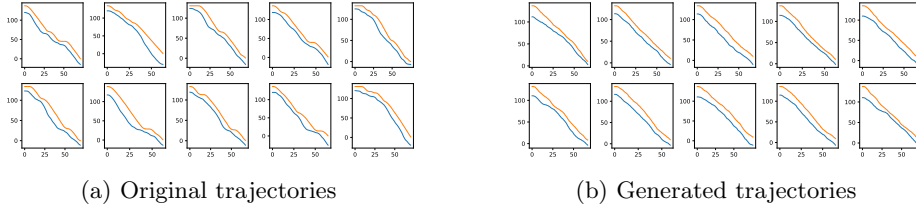


Fig. 5: Original and generated trajectories on Driving dataset. The x-axis is timestamp and y-axis is the location (1D coordinate) of two cars.

## 5.5 Trajectory Generation

The learned copula can also be used to generate new trajectories. We visualize the result of trajectory generation on RoboCup dataset. As shown in Fig. 4, the dotted lines denote the ground-truth trajectories of the 10 player in an attack from midfield to the penalty area. The trajectories generated by our copula model (Fig. 4b) are quite similar to the demonstration as they exhibit high consistency. It is clear that midfielders and forwards (No. 5 ~ No. 11) are basically moving to the same direction, and they all make a left turn on their way to penalty area. However, the generated trajectories by independent modeling show little correlation since the players are all making independent decisions.

We also present the result of trajectory generation on Driving dataset. We randomly select 10 original trajectories and 10 trajectories generated by our method, and visualize the result in Fig. 5. The x-axis is timestamp and y-axis is the location (coordinate) of two cars. Our learned policy is shown to be able to maintain the distance between two cars.

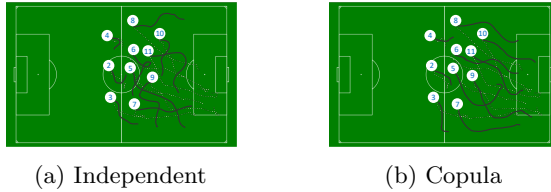


Fig. 4: Generated trajectories (solid lines) on RoboCup using independent modeling or copula. Dotted lines are ground-truth trajectories.

## 6 Conclusion and Future Work

In this paper, we propose a copula-based multi-agent imitation learning algorithm that is interpretable, efficient and scalable to model complex multi-agent interactions. Sklar’s theorem allows us to separately learn marginal policies that capture the local behavioral patterns of each individual agent and a copula function that only and fully captures the dependence structure among the agents. Compared to previous multi-agent imitation learning methods based on independent policies (mean-field factorization of the joint policy) or opponent modeling, our method is capable of modeling complex dependence among agents and achieving coordination without any modeling redundancy.

We point out two directions of future work. First, the copula function is generalizable only if the dependence structure of agents (i.e., their role assignment) is unchanged. Therefore, it is interesting to study how to efficiently apply the learned copula to the scenario with evolving dependence structure. Another practical question is that whether our proposed method can be extended to the setting of decentralized execution, since the step of copula sampling (line 3 or 5 in Algorithm 2) is shared by all agents. A straightforward solution is to set a fixed sequence of random seeds for all agents in advance, so that the copula samples obtained by all agents are the same at each timestamp, but how to design a more robust and elegant mechanism is still a promising direction.

## Acknowledgements

This research was supported by TRI, NSF (1651565, 1522054, 1733686), ONR (N00014-19-1-2145), AFOSR (FA9550-19-1-0024), ARO (W911NF2110125), and FLI.

## References

1. A. Alahi, K. Goel, V. Ramanathan, A. Robicquet, L. Fei-Fei, and S. Savarese. Social lstm: Human trajectory prediction in crowded spaces. In *Proceedings of the IEEE conference on computer vision and pattern recognition*, pages 961–971, 2016.
2. S. V. Albrecht and P. Stone. Autonomous agents modelling other agents: A comprehensive survey and open problems. *Artificial Intelligence*, 258:66–95, 2018.
3. P. Battaglia, R. Pascanu, M. Lai, D. J. Rezende, et al. Interaction networks for learning about objects, relations and physics. In *Advances in neural information processing systems*, pages 4502–4510, 2016.
4. R. P. Bhattacharyya, D. J. Phillips, B. Wulfe, J. Morton, A. Kuefler, and M. J. Kochenderfer. Multi-agent imitation learning for driving simulation. In *2018 IEEE/RSJ International Conference on Intelligent Robots and Systems (IROS)*, pages 1534–1539. IEEE, 2018.
5. E. Bouyé, V. Durrleman, A. Nikeghbali, G. Riboulet, and T. Roncalli. Copulas for finance—a reading guide and some applications. *Available at SSRN 1032533*, 2000.
6. N. Brown and T. Sandholm. Superhuman ai for multiplayer poker. *Science*, 365(6456):885–890, 2019.
7. T. Chu, J. Wang, L. Codecà, and Z. Li. Multi-agent deep reinforcement learning for large-scale traffic signal control. *IEEE Transactions on Intelligent Transportation Systems*, 21(3):1086–1095, 2019.
8. R. A. Davis, K.-S. Lii, and D. N. Politis. Remarks on some nonparametric estimates of a density function. In *Selected Works of Murray Rosenblatt*, pages 95–100. Springer, 2011.
9. A. Dosovitskiy, G. Ros, F. Codevilla, A. Lopez, and V. Koltun. CARLA: An open urban driving simulator. In *Proceedings of the 1st Annual Conference on Robot Learning*, pages 1–16, 2017.
10. J. Fu, K. Luo, and S. Levine. Learning robust rewards with adversarial inverse reinforcement learning. *arXiv preprint arXiv:1710.11248*, 2017.

11. J. Ho and S. Ermon. Generative adversarial imitation learning. In *Advances in neural information processing systems*, pages 4565–4573, 2016.
12. Y. Hoshen. Vain: Attentional multi-agent predictive modeling. In *Advances in Neural Information Processing Systems*, pages 2701–2711, 2017.
13. B. Ivanovic, E. Schmerling, K. Leung, and M. Pavone. Generative modeling of multimodal multi-human behavior. In *2018 IEEE/RSJ International Conference on Intelligent Robots and Systems (IROS)*, pages 3088–3095. IEEE, 2018.
14. H. Joe. *Dependence modeling with copulas*. Chapman and Hall/CRC, 2014.
15. T. N. Kipf, E. Fetaya, K.-C. Wang, M. Welling, and R. S. Zemel. Neural relational inference for interacting systems. In *International Conference on Machine Learning*, 2018.
16. H. M. Le, Y. Yue, P. Carr, and P. Lucey. Coordinated multi-agent imitation learning. In *Proceedings of the 34th International Conference on Machine Learning*, pages 1995–2003, 2017.
17. M. G. Li, B. Jiang, H. Zhu, Z. Che, and Y. Liu. Generative attention networks for multi-agent behavioral modeling. In *AAAI*, pages 7195–7202, 2020.
18. M. L. Littman. Markov games as a framework for multi-agent reinforcement learning. In *Machine learning proceedings 1994*, pages 157–163. Elsevier, 1994.
19. M. Liu, M. Zhou, W. Zhang, Y. Zhuang, J. Wang, W. Liu, and Y. Yu. Multi-agent interactions modeling with correlated policies. *arXiv preprint arXiv:2001.03415*, 2020.
20. O. Michael, O. Obst, F. Schmiddsberger, and F. Stolzenburg. Robocupsimdata: A robocup soccer research dataset. *arXiv preprint arXiv:1711.01703*, 2017.
21. R. B. Nelsen. *An introduction to copulas*. Springer Science & Business Media, 2007.
22. A. Y. Ng, S. J. Russell, et al. Algorithms for inverse reinforcement learning. In *Icml*, volume 1, page 2, 2000.
23. E. Parzen. On estimation of a probability density function and mode. *The annals of mathematical statistics*, 33(3):1065–1076, 1962.
24. D. A. Pomerleau. Efficient training of artificial neural networks for autonomous navigation. *Neural computation*, 3(1):88–97, 1991.
25. M. L. Puterman. *Markov decision processes: discrete stochastic dynamic programming*. John Wiley & Sons, 2014.
26. S. Russell. Learning agents for uncertain environments. In *Proceedings of the eleventh annual conference on Computational learning theory*, pages 101–103, 1998.
27. D. Silver, J. Schrittwieser, K. Simonyan, I. Antonoglou, A. Huang, A. Guez, T. Hubert, L. Baker, M. Lai, A. Bolton, et al. Mastering the game of go without human knowledge. *nature*, 550(7676):354–359, 2017.
28. A. Sklar. Fonctions de Répartition à n Dimensions et Leurs Marges. *Publications de L’Institut de Statistique de L’Université de Paris*, 8:229–231, 1959.
29. M. Sklar. Fonctions de répartition an dimensions et leurs marges. *Publ. inst. statist. univ. Paris*, 8:229–231, 1959.
30. J. Song, H. Ren, D. Sadigh, and S. Ermon. Multi-agent generative adversarial imitation learning. In *Advances in neural information processing systems*, pages 7461–7472, 2018.
31. S. Sukhbaatar, R. Fergus, et al. Learning multiagent communication with backpropagation. In *Advances in neural information processing systems*, pages 2244–2252, 2016.
32. U. Syed, M. Bowling, and R. E. Schapire. Apprenticeship learning using linear programming. In *Proceedings of the 25th international conference on Machine learning*, pages 1032–1039, 2008.



33. Z. Tian, Y. Wen, Z. Gong, F. Punakkath, S. Zou, and J. Wang. A regularized opponent model with maximum entropy objective. *arXiv preprint arXiv:1905.08087*, 2019.
34. R. A. Yeh, A. G. Schwing, J. Huang, and K. Murphy. Diverse generation for multi-agent sports games. In *Proceedings of the IEEE Conference on Computer Vision and Pattern Recognition*, pages 4610–4619, 2019.
35. L. Yu, J. Song, and S. Ermon. Multi-agent adversarial inverse reinforcement learning. In *International Conference on Machine Learning*, 2019.
36. E. Zhan, S. Zheng, Y. Yue, L. Sha, and P. Lucey. Generating multi-agent trajectories using programmatic weak supervision. *arXiv preprint arXiv:1803.07612*, 2018.

## Appendix

### A Dataset Details

**PhySim** is collected from a physical simulation environment where 5 particles move in a unit 2D box. The state is locations of all particles and the action is their acceleration (there is no need to include their velocities in state because accelerations are completely determined by particle locations). We add Gaussian noise to the observed values of actions. Particles may be pairwise connected by springs, which can be represented as a binary adjacency matrix  $\mathbf{A} \in \{0, 1\}^{N \times N}$ . The elasticity between two particles scales linearly with their distance. At each timestamp, we randomly sample an adjacency matrix from  $\{\mathbf{A}_1, \mathbf{A}_2\}$  to connect all particles, where  $\mathbf{A}_1$  and  $\mathbf{A}_2$  are set as complimentary (i.e.  $\mathbf{A}_1 + \mathbf{A}_2 + \mathbf{I} = \mathbf{1}$ ) to ensure that they are as different as possible. Therefore, the marginal action distribution of each particle given a system state is Gaussian mixtures with two components. Here the coordination signal for particles can be seen as the hidden variable determining which set of springs ( $\mathbf{A}_1$  or  $\mathbf{A}_2$ ) is used at current time. We generate 10,000 training trajectories, 2,000 validation trajectories, and 2,000 test trajectories for experiments, where the length of each trajectory is 500.

**Driving** is generated by CARLA<sup>3</sup> [9], an open-source simulator for autonomous driving research that provides realistic urban environments for training and validation of autonomous driving systems. To generate the driving data, we design a car following scenario, where a leader car and a follower car drive in the same lane. We make the leader car alternatively accelerate to a speed upper bound and slow down to stopping. The leader car does not care about the follower and drives following its own policy. The follower car tries to follow closely the leader car while keeping a safe distance. Here the state is the locations and velocities of the two cars, and the action is their accelerations. We generate 1,009 trajectories in total, and split the whole data into training, validation, and test set with ratio of 6 : 2 : 2. The average length of trajectories is 85.5 in Driving dataset.

**RoboCup** [20] is collected from an international scientific robot football competition in which teams of multiple robots compete against each other. The original dataset contains all pairings of 10 teams with 25 repetitions of each game (1,125 games in total). The state of a game (locations and velocities of 22 robots) is recorded every 100 ms, resulting in a trajectory of length 6,000 for each game (10 min). We select the 25 games between two teams, cyrus2017 and helios2017, as the data used in this paper. The state is locations of 10 robots (except the goalkeeper) in the left team, and the action is their velocities. The dataset is split into training, validation, and test set with ratio of 6 : 2 : 2.

### B Implementation Details

For our proposed method, to learn the marginal action distribution of each agent (i.e. Gaussian mixtures), we use an MLP with one hidden layer to take as input

<sup>3</sup> <https://carla.org/>

a state and output the centers of their Gaussian mixtures. To prevent overfitting, the variance of these Gaussian mixtures is parameterized by a free variable for each particle, and the weights of mixtures are set as uniform. Each dimension of states and actions in the original datasets are normalized to range  $[-1, 1]$ . For PhySim, the number of particles are set to 5. Learning rate is set to 0.01, and the weight of L2 regularizer is set to  $10^{-5}$ . For Driving, learning rate is 0.005 and L2 regularizer weight is  $10^{-5}$ . For RoboCup, learning rate is 0.001 and L2 regularizer weight is  $10^{-6}$ .

For LR, we use the default implementation in Python sklearn package. For SocialLSTM [1], the dimension of input is set as the dimension of states in each dataset. The spatial pooling size is 32, and we use an  $8 \times 8$  sum pooling window size without overlaps. The hidden state dimension in LSTM is 128. The learning rate is 0.001. For IN [3], all MLPs are with one hidden layer of 32 units. The learning rate is 0.005. For CommNet [31], all MLPs are with one hidden layer of 32 units. The dimension of hidden states is set to 64, and the number of communication round is set to 2. The learning rate is 0.001. For VAIN [12], the encoder and decoder functions are implemented as a fully connected neural network with one hidden layer of 32 units. The dimension of hidden states is 64, and the dimension of attention vectors is 10. The learning rate is 0.0005. For NRI [15], we use an MLP encoder and an MLP decoder, with one hidden layer of 32 units. The learning rate is 0.001.